

Improving the stimulated Raman adiabatic passage via dissipative quantum dynamics

Qi-Cheng Wu,¹ Ye-Hong Chen,¹ Bi-Hua Huang,¹ Jie Song,² Yan Xia,^{1,*} Shi-Biao Zheng¹

¹*Department of Physics, Fuzhou University, Fuzhou 350002, China*

²*Department of Physics, Harbin Institute of Technology, Harbin 150001, China**

We propose a method to improve the stimulated Raman adiabatic passage (STIRAP) via dissipative quantum dynamics, taking into account the dephasing effects. Fast and robust population transfer can be obtained with the scheme by the designed pulses and detuning, even though the initial state of the system is imperfect. With a concrete three-level system as an example, the influences of the imperfect initial state, variations in the control parameters, and various dissipation effects are discussed in detail. The numerical simulation shows that the scheme is insensitive to moderate fluctuations of experimental parameters and the relatively large dissipation effects of the excited state. Furthermore, the dominant dissipative factors, namely, the dephasing effects of the ground states and the imperfect initial state are no longer undesirable, in fact, they are the important resources to the scheme. Therefore, the scheme could provide more choices for the realization of the complete population transfer in the strong dissipative fields where the standard stimulated Raman adiabatic passage or shortcut schemes are invalid.

PACS numbers:

Keywords: (270.0270) Quantum optics; (270.2500) Fluctuations, relaxations, and noise; (270.5585) Quantum information and processing.

-
- [1] S. Barz, J. F. Fitzsimons, E. Kashefi, and P. Walther, “Experimental verification of quantum computation,” *Nat. Phys.* **9**(11), 727–731 (2013).
 - [2] M. O. Scully, *Quantum Optics* (Cambridge University Press, Cambridge, 1997).
 - [3] M. Kasevich, “Coherence with atoms,” *Science* **298**(5597), 1363–1368 (2002).
 - [4] K. Kotru, D. L. Butts, J. M. Kinast, and R. E. Stoner, “Large-Area Atom Interferometry with Frequency-Swept Raman Adiabatic Passage,” *Phys. Rev. Lett.* **115**(10), 103001 (2015).
 - [5] U. Gaubatz, P. Rudecki, S. Schiemann, and K. Bergmann, “Population transfer between molecular vibrational levels by stimulated Raman scattering with partially overlapping laser fields. A new concept and experimental results,” *J. Chem. Phys.* **92**(9), 5363–5376 (1990).
 - [6] K. Bergmann, H. Theuer, and B. W. Shore, “Coherent population transfer among quantum states of atoms and molecules,” *Rev. Mod. Phys.* **70**(3), 1003 (1998).
 - [7] N. V. Vitanov, M. Fleischhauer, B. W. Shore, and K. Bergmann, “Coherent manipulation of atoms and molecules by sequential laser pulses,” *Adv. At. Mol. Opt. Phys.* **46**, 55–190 (2001).
 - [8] M. Demirplak and S. A. Rice, “Adiabatic population transfer with control fields,” *J. Phys. Chem. A* **107**(46), 9937–9945 (2003).
 - [9] L. Giannelli and E. Arimondo, “Three-level superadiabatic quantum driving,” *Phys. Rev. A* **89**(3), 033419 (2014).
 - [10] Y. Sun and H. Metcalf, “Nonadiabaticity in stimulated Raman adiabatic passage,” *Phys. Rev. A* **90**(3), 033408 (2014).
 - [11] M. Demirplak and S. A. Rice, “Optical control of molecular dynamics in a liquid,” *J. Chem. Phys.* **116**(18), 8028–8035 (2002).
 - [12] P. A. Ivanov, N. V. Vitanov, and K. Bergmann, “Effect of dephasing on stimulated Raman adiabatic passage,” *Phys. Rev. A* **70**(6), 063409 (2004).
 - [13] X. Lacour, S. Guérin, and H. R. Jauslin, “Optimized adiabatic passage with dephasing,” *Phys. Rev. A* **78**(3), 033417 (2008).
 - [14] X. J. Lu, X. Chen, A. Ruschhaupt, D. Alonso, S. Guerin, and J. G. Muga, “Fast and robust population transfer in two-level quantum systems with dephasing noise and/or systematic frequency errors,” *Phys. Rev. A* **88**(3), 033406 (2013).
 - [15] Y. H. Issoufa and A. Messikh, “Effect of dephasing on superadiabatic three-level quantum driving,” *Phys. Rev. A* **90**(5), 055402 (2014).
 - [16] E.-M. Graefe, A. A. Mailybaev, and N. Moiseyev, “Breakdown of adiabatic transfer of light in waveguides in the presence of absorption,” *Phys. Rev. A* **88**(7), 033842 (2013).
 - [17] K. S. Kumar, A. Vepsäläinen, S. Danilin, and G. S. Paraoanu, “Stimulated Raman adiabatic passage in a three-level superconducting circuit,” *Nat. Commun.* **7**, 10628 (2016).

*Electronic address: *xia-208@163.com

- [18] M. Demirplak and S. A. Rice, “Adiabatic population transfer with control fields,” *J. Phys. Chem. A* **107**(46), 9937–9945 (2003); “On the consistency, extremal, and global properties of counterdiabatic fields,” *J. Chem. Phys.* **129**(15), 154111 (2008).
- [19] M. V. Berry, “Transitionless quantum driving,” *J. Phys. A* **42**(36), 365303 (2009).
- [20] A. del Campo, M. M. Rams, and W. H. Zurek, “Assisted finite-rate adiabatic passage across a quantum critical point: Exact solution for the quantum Ising model,” *Phys. Rev. Lett.* **109**(11), 115703 (2012); H. Saberi, T. Opatrný, K. Mølmer, and A. del Campo, “Adiabatic tracking of quantum many-body dynamics,” *Phys. Rev. A* **90**(6), 060301(R) (2014).
- [21] Y. H. Chen, Y. Xia, J. Song, and B. H. Huang, “Shortcuts to adiabatic passage for fast generation of Greenberger-Horne-Zeilinger states by transitionless quantum driving,” *Sci. Rep.* **5**, 15616 (2015).
- [22] Z. Chen, Y. H. Chen, Y. Xia, J. Song, and B. H. Huang, “Fast generation of three-atom singlet state by transitionless quantum driving,” *Sci. Rep.* **6**, 22202 (2016).
- [23] M. Lu, Y. Xia, L. T. Shen, J. Song, and N. B. An, “Shortcuts to adiabatic passage for population transfer and maximum entanglement creation between two atoms in a cavity,” *Phys. Rev. A* **89**(1), 012326 (2014).
- [24] X. Chen, E. Torrontegui, and J. G. Muga, “Lewis-Riesenfeld invariants and transitionless quantum driving,” *Phys. Rev. A* **83**(6), 062116 (2011); X. Chen and J. G. Muga, “Engineering of fast population transfer in three-level systems,” *Phys. Rev. A* **86**(3), 033405 (2012).
- [25] Y. H. Chen, Y. Xia, Q. Q. Cheng, and J. Song, “Fast and noise-resistant implementation of quantum phase gates and creation of quantum entangled states,” *Phys. Rev. A* **91**(1), 012325 (2015).
- [26] Y. H. Chen, Y. Xia, Q. Q. Cheng, and J. Song, “Shortcuts to adiabatic passage for multiparticles in distant cavities: applications to fast and noise-resistant quantum population transfer, entangled states preparation and transition,” *Laser. Phys. Lett.* **11**(11), 115201 (2014).
- [27] Y. H. Chen, Y. Xia, Q. Q. Cheng, and J. Song, “Efficient shortcuts to adiabatic passage for fast population transfer in multiparticle systems,” *Phys. Rev. A* **89**(3), 033856 (2014).
- [28] G. Dridi, S. Guérin, V. Hakobyan, H. R. Jauslin, and H. Eleuch, “Ultrafast stimulated Raman parallel adiabatic passage by shaped pulses,” *Phys. Rev. A* **80**(4), 043408 (2009).
- [29] X. Chen, I. Lizuain, A. Ruschhaupt, D. Guery-Odelin, and J. G. Muga, “Shortcut to adiabatic passage in two- and three-level atoms,” *Phys. Rev. Lett.* **105**(12), 123003 (2010).
- [30] B. T. Torosov, S. Guérin, and N. V. Vitanov, “High-fidelity adiabatic passage by composite sequences of chirped pulses,” *Phys. Rev. Lett.* **106**(23), 233001 (2011).
- [31] A. del Campo, “Frictionless quantum quenches in ultracold gases: A quantum-dynamical microscope,” *Phys. Rev. A* **84**(3), 031606 (2011); “Shortcuts to adiabaticity by counterdiabatic driving,” *Phys. Rev. Lett.* **111**(10), 100502 (2013).
- [32] Y. H. Chen, Y. Xia, Q. C. Wu, B. H. Huang, and J. Song, “Method for constructing shortcuts to adiabaticity by a substitute of counterdiabatic driving terms,” *Phys. Rev. A* **93**(5), 052109 (2016).
- [33] S. Ibáñez, X. Chen, and J. G. Muga, “Improving shortcuts to adiabaticity by iterative interaction pictures,” *Phys. Rev. A* **87**(4), 043402 (2013).
- [34] S. Martínez-Garaot, E. Torrontegui, X. Chen, and J. G. Muga, “Shortcuts to adiabaticity in three-level systems using Lie transforms,” *Phys. Rev. A* **89**(5), 053408 (2014).
- [35] F. Verstraete, M. M. Wolf, and J. I. Cirac, “Quantum computation and quantum-state engineering driven by dissipation,” *Nature Phys.* **5**(9), 633–636 (2009).
- [36] G. Vacanti and A. Beige, “Cooling atoms into entangled states,” *New J. Phys.* **11**(8), 083008 (2009).
- [37] M. J. Kastoryano, F. Reiter, and A. S. Sørensen, “Dissipative preparation of entanglement in optical cavities,” *Phys. Rev. Lett.* **106**(9), 090502 (2011).
- [38] X. Q. Shao, T. Y. Zheng, and S. Zhang, “Engineering steady three-atom singlet states via quantum-jump-based feedback,” *Phys. Rev. A* **85**(4), 042308 (2012).
- [39] L. T. Shen, X. Y. Chen, Z. B. Yang, H. Z. Wu, and S. B. Zheng, “Steady-state entanglement for distant atoms by dissipation in coupled cavities,” *Phys. Rev. A* **84**(6), 064302 (2011).
- [40] Q. C. Wu and X. Ji, “Generation of steady three- and four-dimensional entangled states via quantum-jump-based feedback,” *Quantum Inf. Process.* **12**(10), 3167–3178 (2013).
- [41] C. M. Bender and S. Boettcher, “Real spectra in non-Hermitian Hamiltonians having PT symmetry,” *Phys. Rev. Lett.* **80**(24), 5243 (1998); C. M. Bender, D. C. Brody, H. F. Jones, and B. K. Meister, “Faster than Hermitian quantum mechanics,” *Phys. Rev. Lett.* **98**(4), 040403 (2007).
- [42] B. T. Torosov, G. D. Valle, and S. Longhi, “Non-Hermitian shortcut to stimulated Raman adiabatic passage,” *Phys. Rev. A* **89**(6), 063412 (2014).
- [43] J. Dalibard, Y. Castin, and K. Mølmer, “Wave-function approach to dissipative processes in quantum optics,” *Phys. Rev. Lett.* **68**(5), 580 (1992).
- [44] M. B. Plenio and P. L. Knight, “The quantum-jump approach to dissipative dynamics in quantum optics,” *Rev. Mod. Phys.* **70**(1), 101 (1998).
- [45] D. Møller, L. B. Madsen, and K. Mølmer, “Geometric phases in open tripod systems,” *Phys. Rev. A* **77**(2), 022306 (2008).
- [46] T. A. Laine and S. Stenholm, “Adiabatic processes in three-level systems,” *Phys. Rev. A* **53**(4), 2501 (1996).
- [47] G. Dattoli, A. Torre, and R. Mignani, “Non-Hermitian evolution of two-level quantum systems,” *Phys. Rev. A* **42**(3), 1467 (1990).
- [48] N. Moiseyev, “Quantum theory of resonances: calculating energies, widths and cross-sections by complex scaling,” *Phys. Rep.* **302**(5), 212–293 (1998).
- [49] J. Okolowicz, M. Płoszajczak, and I. Rotter, “Dynamics of quantum systems embedded in a continuum,” *Phys. Rep.*

- 374**(4), 271–383 (2003).
- [50] M. V. Berry, “Physics of nonhermitian degeneracies,” *Czech. J. Phys.* **54**(10), 1039–1047 (2004).
 - [51] J. Randall, S. Weidt, E. D. Standing, K. Lake, S. C. Webster, D. F. Murgia, T. Navickas, K. Roth, and W. K. Hensinger, “Efficient preparation and detection of microwave dressed-state qubits and qutrits with trapped ions,” *Phys. Rev. A* **91**(1), 012322 (2015).
 - [52] J. G. Muga, J. Echanobe, A. del Campo, and I. Lizuain, “Generalized relation between pulsed and continuous measurements in the quantum Zeno effect,” *J. Phys. B* **41**, 175501 (2008).
 - [53] T. Yu, L. Diósi, N. Gisin, and W. T. Strunz, “Non-Markovian quantum-state diffusion: Perturbation approach,” *Phys. Rev. A* **60**(1), 91 (1999); T. Yu, “Non-Markovian quantum trajectories versus master equations: finite-temperature heat bath,” *Phys. Rev. A* **69**(6), 062107 (2004).
 - [54] J. Jing and T. Yu, “Non-Markovian relaxation of a three-level system: Quantum trajectory approach,” *Phys. Rev. Lett.* **105**(24), 240403 (2010); J. Jing, L. A. Wu, M. S. Sarandy, and J. G. Muga, “Inverse engineering control in open quantum systems,” *Phys. Rev. A* **88**(5), 053422 (2013).
 - [55] S. Maniscalco and F. Petruccione, “Non-Markovian dynamics of a qubit,” *Phys. Rev. A* **73**(1), 012111 (2006).
 - [56] M. G. Bason, M. Viteau, N. Malossi, P. Huillery, E. Arimondo, D. Ciampini, R. Fazio, V. Giovannetti, R. Mannella, and O. Morsch, “High-fidelity quantum driving,” *Nature Phys.* **8**(2), 147–152 (2012).
 - [57] J. Zhang, J. H. Shim, I. Niemeyer, T. Taniguchi, T. Teraji, H. Abe, S. Onoda, T. Yamamoto, T. Ohshima, J. Isoya et al., “Experimental implementation of assisted quantum adiabatic passage in a single spin,” *Phys. Rev. Lett.* **110**(24), 240501 (2013).
 - [58] Y. X. Du, Z. T. Liang, Y. C. Li, X. X. Yue, Q. X. Lv, W. Huang, X. Chen, H. Yan, and S. L. Zhu, “Experimental realization of stimulated Raman superadiabatic passage with cold atoms,” *arXiv:1601.06058*.
 - [59] S. An, D. Lv, A. del Campo, and K. Kim, “Shortcuts to Adiabaticity by Counterdiabatic Driving in Trapped-ion Transport,” *arXiv:1601.05551*.
 - [60] M. V. Berry and R. Uzdin, “Slow non-Hermitian cycling: exact solutions and the Stokes phenomenon,” *J. Phys. A: Math. Theor.* **44**(43), 435303 (2011).
 - [61] A. Leclerc, D. Viennot, and G. Jolicard, “The role of the geometric phases in adiabatic population tracking for non-Hermitian Hamiltonians,” *J. Phys. A: Math. Theor.* **45**(41), 415201 (2012).
 - [62] S. Ibáñez and J. G. Muga, “Adiabaticity condition for non-Hermitian Hamiltonians,” *Phys. Rev. A* **89**(3), 033403 (2014).

I. INTRODUCTION

The ability to accurately control a quantum system is a fundamental requirement in many areas of modern science ranging from quantum information processing [1] and coherent manipulation of quantum systems [2] to high-precision measurements [3, 4]. The technique of stimulated Raman adiabatic passage (STIRAP) offers, in principle, a simple approach for a complete population transfer of a three-level quantum system has already drawn great attention, and the basic properties of the STIRAP have been scrutinized both theoretically and experimentally [5–17]. However, this process requires large pulse areas, i.e., large average Rabi frequencies, and long interaction time. For several applications, this requirement is a critical disadvantage, more specifically, the ideal robustness and the intended dynamics may be spoiled by the vast amount of accumulation of perturbations and decoherence due to noise and undesired interactions.

To overcome this problem, several strategies have been proposed, in which one promising solution to this problem is the shortcuts to adiabaticity dynamics [18–34]. The basic idea of the shortcuts to adiabaticity dynamics is to accelerate the dynamics towards the perfect final outcome so that the accumulation of decoherence effects will be reduced effectively. Based on this novel idea, several methods have been proposed, such as counter-diabatic driving (equivalently, the transitionless quantum algorithm) [18–21, 23], Lewis-Riesenfeld inverse engineering [24–27], parallel adiabatic passage [28], and so on. Those methods imply a strict time dependence of the pulses or detuning. One can use the constructed composite pulses to improve dramatically the fidelity of the adiabatic passage [18–34]. For example, based on the transitionless quantum driving, Chen *et al.* have proposed a shortcut to the STIRAP with auxiliary pulses, which could provide a fast and robust approach to population control [29]. However, some dissipative effects (e.g., the dephasing) [11–16] still produce significant negative effects on the schemes with above methods. In addition, it is a pity that there has been a long lack of studies on the impact on the imperfect initial conditions which may occur in the experiment. Therefore, the shortcuts to adiabaticity dynamics will also be limited severely by the presence of the strong dissipation effects and imperfect initial conditions.

Besides the shortcuts to adiabaticity dynamics, another popular approach, so-called dissipative quantum dynamics (DQD) [35–37], also work well for coping with the dissipative effects. In fact, several authors have pointed out that it is possible to generate entanglement based on dissipative quantum dynamical process [38–40]. The basic idea of the DQD can be summarized as follows: the interaction of the system with the environment is employed such that the target state becomes the stationary state of the system. In other words, some specific dissipative factors are no longer undesirable, but can be regarded as the important resources. This idea is consistent with the results in Ref. [41]

where Bender has elaborated that a \mathcal{PT} -symmetric Hamiltonian can produce a faster-than-Hermitian evolution in a two-state quantum system, while keeping the eigenenergy difference fixed. Recently, Torosov *et al.* have proposed a non-Hermitian generalization of STIRAP, which allows one to increase speed and fidelity of the adiabatic passage [42]. However, the so-called non-Hermitian shortcut is very sensitive to the initial conditions, and the intermediate excited state always exists and couldn't be neglected, which may be limited severely by the presence of the dissipation effects of the excited state. In particular, Issoufa *et al.* have found that the dephasing effects will reduce the performance of the population transfer and the fidelity can be far below the quantum computation target even for small dephasing rates [15]. Thus, it is very worthwhile to find an effective way to circumvent various dissipative factors or the imperfect initial conditions which may occur in the experiment.

In this paper, taking into account various decoherence factors (such as the imperfect initial conditions, the dephasing and damping effects, and the variations in the control parameters), we aim at designing the pulses and detuning to increase the speed and robustness of STIRAP by cutting off some coupling transitions via the DQD. The scheme has the following advantages: (1) Unlike the previous STIRAP or shortcut schemes [5–15, 24, 29], the dominant dissipative factors are no longer undesirable, in fact, they are the important resources to the scheme. (2) By the designed pulses and detuning, the target state will become the stationary state of the system approximatively. Then, even though the initial state is imperfect, the actual state will also follow the evolution of the target state closely, thereby a complete population transfer will be achieved fast and efficiently. (3) The scheme is insensitive to the moderate fluctuations of experimental parameters and the relatively large dissipation effects of the excited state. (4) The approach makes it possible to improve the speed of the system evolution in strong dissipative fields where the standard STIRAP or shortcut schemes are invalid.

The rest of this paper is arranged as follows. In Sec. II, we briefly analyse the dynamics of the STIRAP process with the quantum jump approach [43–45], the mechanism of the population transfer in STIRAP and the limitation of adiabaticity can be easily obtained. In Sec. III, taking into account the dephasing effects of the ground states, the dynamics for the three-level system is also analysed with the quantum jump approach. With the help of DQD, the pulses and detuning design strategies are put forward. Then, we consider a concrete three-level system example to show the usefulness of the engineering method, the pulses and detuning shapes for the constant dephasing rate are discussed in detail. Sec. IV reports numerical analyses of the scheme. Population engineering, the influences of fluctuations of experimental parameters and the dissipation effects of the excited state, are discussed step by step. We conclude with a summary of the scheme in Sec. V.

II. THE DYNAMICS OF THE STIRAP PROCESS

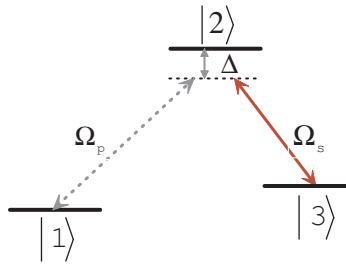


FIG. 1: Three-level Λ system driven by two coherent fields, a pump (Stokes) field with Rabi frequency Ω_p (Ω_s). The two fields have the same detuning Δ , where the time dependence has been omitted for convenience.

In this section we briefly review the theory behind the STIRAP process for the three-state systems. Let us consider a single-photon detuning three-level quantum system in a Λ configuration system as shown in Fig. 1. The excited state is labelled as $|2\rangle$ and two ground states are $|1\rangle$ and $|3\rangle$. The transition between the levels $|1\rangle \leftrightarrow |2\rangle$ is driven by the pump pulse detuned from resonance by $\Delta(t)$ with the Rabi frequency $\Omega_p(t)$. Whereas, the transition between the $|2\rangle \leftrightarrow |3\rangle$ is driven by the Stokes pulse detuned from resonance by $\Delta(t)$ with the Rabi frequency $\Omega_s(t)$. The dipole transition $|1\rangle \leftrightarrow |3\rangle$ is a forbidden transition. In the absence of decoherence, the dynamics of the system is governed by the Schrödinger equation ($\hbar = 1$)

$$i\dot{c}(t) = H_0(t)c(t), \quad (1)$$

where the vector $c(t)=[c_1(t), c_2(t), c_3(t)]^T$ contains the three probability amplitudes of states $|1\rangle$, $|2\rangle$, and $|3\rangle$. The

Hamiltonian within the rotating wave approximation [2] reads as

$$H_0(t) = \frac{1}{2} \begin{pmatrix} 0 & \Omega_p(t) & 0 \\ \Omega_p(t) & 2\Delta(t) & \Omega_s(t) \\ 0 & \Omega_s(t) & 0 \end{pmatrix}. \quad (2)$$

The instantaneous eigenvalues of the Hamiltonian $H_0(t)$ are given by

$$\lambda_+(t) = \frac{\Omega_0(t) \cot \phi(t)}{2}, \quad \lambda_0(t) = 0, \quad \lambda_-(t) = \frac{-\Omega_0(t) \tan \phi(t)}{2}, \quad (3)$$

where $\Omega_0(t)$ and the mixing angle $\phi(t)$ are, respectively, defined by

$$\Omega_0(t) = \sqrt{\Omega_p(t)^2 + \Omega_s(t)^2}, \quad \tan \phi(t) = \frac{\Omega_0(t)}{\Delta(t) + \sqrt{\Delta(t)^2 + \Omega_0(t)^2}}, \quad (4)$$

with

$$\dot{\phi}(t) = \frac{\dot{\Omega}_0(t)\Delta(t) - \Omega_0(t)\dot{\Delta}(t)}{2(\Delta(t)^2 + \Omega_0(t)^2)}. \quad (5)$$

Their corresponding eigenstates are given by the following adiabatic states [6]

$$\begin{aligned} |a_+(t)\rangle &= \sin \theta(t) \sin \phi(t) |1\rangle + \cos \phi(t) |2\rangle + \cos \theta(t) \sin \phi(t) |3\rangle, \\ |a_0(t)\rangle &= \cos \theta(t) |1\rangle - \sin \theta(t) |3\rangle, \\ |a_-(t)\rangle &= \sin \theta(t) \cos \phi(t) |1\rangle - \sin \phi(t) |2\rangle + \cos \theta(t) \cos \phi(t) |3\rangle, \end{aligned} \quad (6)$$

where the mixing angle $\theta(t)$ is defined by

$$\tan \theta(t) = \frac{\Omega_p(t)}{\Omega_s(t)}, \quad \dot{\theta}(t) = \frac{\dot{\Omega}_p(t)\Omega_s(t) - \Omega_p(t)\dot{\Omega}_s(t)}{\Omega_0(t)^2}. \quad (7)$$

We can find that the eigenstate $|a_0(t)\rangle$ is a dark state with zero projection on state $|2\rangle$, which is available for the effective population transfer. It is advisable to project the Schrödinger equation into the so-called adiabatic states $\{|a_+(t)\rangle, |a_0(t)\rangle, |a_-(t)\rangle\}$. The probability amplitudes of the adiabatic states $a(t)=[a_+(t), a_0(t), a_-(t)]^T$ are connected to the original ones by using the transformation

$$c(t) = R(t)a(t), \quad (8)$$

where the transformation matrix R is given by

$$R(t) = \begin{pmatrix} \sin \theta(t) \sin \phi(t) & \cos \theta(t) & \sin \theta(t) \cos \phi(t) \\ \cos \phi(t) & 0 & -\sin \phi(t) \\ \cos \theta(t) \sin \phi(t) & -\sin \theta(t) & \cos \theta(t) \cos \phi(t) \end{pmatrix}. \quad (9)$$

The Schrödinger equation in the adiabatic basis can be written as

$$i\dot{a}(t) = H_0^a a(t), \quad (10)$$

with $H_0^a = R(t)^{-1}H_0(t)R(t) - iR(t)^{-1}\dot{R}(t)$ or, explicitly,

$$H_0^a = \begin{pmatrix} \lambda_+(t) & \Omega_1^*(t) & \Omega_3^*(t) \\ \Omega_1(t) & 0 & \Omega_2^*(t) \\ \Omega_3(t) & \Omega_2(t) & \lambda_-(t) \end{pmatrix}, \quad (11)$$

where

$$\Omega_1(t) = -i\dot{\theta}(t) \sin \phi(t), \quad \Omega_2(t) = i\dot{\theta}(t) \cos \phi(t), \quad \Omega_3(t) = -i\dot{\phi}(t). \quad (12)$$

In order to gain a qualitative understanding of the STIRAP process, we now use the quantum jump approach [43–45] to analyse current system as shown in Fig. 2. We can easily find that the STIRAP process can be considered as a three-level toy model driven by three effective coherent fields $\Omega_1(t)$, $\Omega_2(t)$, and $\Omega_3(t)$. When

$$|\Omega_1(t)| \ll |\lambda_+(t)|, |\Omega_2(t)| \ll |\lambda_-(t)|, |\Omega_3(t)| \ll |\lambda_+(t) - \lambda_-(t)|, \quad (13)$$

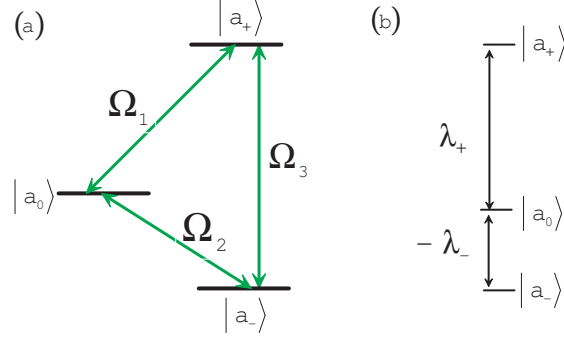


FIG. 2: (a) Effective level scheme of the STIRAP process driven by three effective coherent fields $\Omega_1(t)$, $\Omega_2(t)$, and $\Omega_3(t)$. (b) The energy difference between the adiabatic states $|a_+(t)\rangle$ and $|a_0(t)\rangle$ ($|a_0(t)\rangle$ and $|a_-(t)\rangle$) is given by λ_+ ($-\lambda_-$).

the transitions between the adiabatic states will be greatly suppressed due to the rapid oscillations. In other words, when the Eq. (13) is satisfied, if the system is initially in one of the adiabatic states, then it stays in the adiabatic state during the evolution. More specifically, the initially populated state is $|\psi(0)\rangle = |1\rangle$, and it coincides with $|a_0(t)\rangle$ for $\theta(t) \approx 0$, which can be realized with the counterintuitive pulses order [6–9, 46]. For a counterintuitive order of the pump and Stokes pulses, we have the relations

$$\tan \theta(t) \xrightarrow{t \rightarrow t_i} 0, \tan \theta(t) \xrightarrow{t \rightarrow t_f} \infty, \quad (14)$$

where t_i (t_f) is the initial (final) time for the counterintuitive pulses. Then, as time evolves, the mixing angle $\theta(t)$ rises from 0 to $\pi/2$, and we achieve a complete population transfer

$$|a_0(t_i)\rangle = |1\rangle \longrightarrow |a_0(t_f)\rangle = -|3\rangle. \quad (15)$$

Here, we should note that above derivations are based on the ideal cases, namely perfect adiabaticity, perfect initial state, and without the decoherence effects. However, the perfect adiabaticity in Eq. (13) always means long evolution time which is never experimentally possible nor theoretically expected. Therefore, some nonadiabatic couplings $\Omega_1(t)$ and $\Omega_2(t)$ are always present, which limits the efficiency of STIRAP. Furthermore, the imperfect of initial state and the decoherence effects also have negative effects on the system. Another point which is important to stress is that the coupling term $\Omega_3(t)$ between $|a_+(t)\rangle$ and $|a_-(t)\rangle$, seems not necessary for a full passage from $|1\rangle$ to $|3\rangle$ in principle. For the purpose of convenience, in several of the published numerical calculations of the STIRAP process [9, 10, 42], $\dot{\phi}(t)$ are vanished in the interesting case of $\Delta(t) = \eta\Omega_0(t)$. Here, η can be any constant, also zero, leading to the convenient choice $\Delta(t) = 0$. However, in the scheme, the detuning $\Delta(t)$ plays a important role in the presence of dephasing effects and imperfect initial conditions.

III. DISSIPATIVE QUANTUM DYNAMICS SHORTCUT

According to the DQD, the decoherence effects in the system should be employed as far as possible to improve the STIRAP process. For the standard STIRAP process, the dissipation effects of the ground states may be the dominant source of decoherence, since the system always stays in $|a_0(t)\rangle$ which is constituted by two ground states during the evolution. Therefore, in the following discussion, we will concentrate on the dissipation effects of the ground states. Other dissipation effects including the radiation processes and the dephasing effect of the excited state $|2\rangle$, are considered as the perturbations, we will discuss their impacts on the scheme in the Sec. IV.

In general, for the dissipative quantum systems, the complex energies with negative imaginary parts are used to describe an overall probability decrease that models decay, transport, or scattering phenomena (see, e.g., Refs. [47–50] and references therein). Here, without loss of generality, we consider the dissipation effects of the ground states with the form [42, 51]

$$H_I = -i\frac{\Gamma(t)}{2}[|1\rangle\langle 1| - |3\rangle\langle 3|], \quad (16)$$

where $-i\Gamma(t)/2$ correspond to time-varying complex energies of the bare states $|1\rangle$ and $|3\rangle$, which may be induced by environmental effects or the fluctuating frequencies of the control fields. In fact, similar dissipation effects are widely

discussed in Refs. [9–15], and such dissipation effects can be considered as the dephasing effects which occur in the experiment due to the collisions or phase fluctuations of the control fields. In the following, we will show how to achieve a complete population transfer in a short time with such “dephasing effects”.

A. Pulses and detuning design strategy

Taking into account the dephasing effects of the ground states, the Hamiltonian of the system can be rewritten as

$$H_{\Gamma(t)} = H_0 + H_I = \frac{\hbar}{2} \begin{pmatrix} -i\Gamma(t) & \Omega_p(t) & 0 \\ \Omega_p(t) & 2\Delta(t) & \Omega_s(t) \\ 0 & \Omega_s(t) & i\Gamma(t) \end{pmatrix}. \quad (17)$$

In the adiabatic basis Eq. (6), this Hamiltonian has the form

$$H_{\Gamma(t)}^a = \begin{pmatrix} \Omega_{++}(t) & \Omega_{+0}(t) & \Omega_{+-}(t) \\ \Omega_{0+}(t) & \Omega_{00}(t) & \Omega_{0-}(t) \\ \Omega_{-+}(t) & \Omega_{-0}(t) & \Omega_{--}(t) \end{pmatrix}, \quad (18)$$

where

$$\begin{aligned} \Omega_{++}(t) &= \lambda_+(t) + i \frac{\Gamma \cos 2\theta(t) \sin^2 \phi(t)}{2}, & \Omega_{+0}(t) &= i\dot{\theta}(t) \sin \phi(t) - i \frac{\Gamma \sin 2\theta(t) \sin \phi(t)}{2}, \\ \Omega_{+-}(t) &= i\dot{\phi}(t) + i \frac{\Gamma \cos 2\theta(t) \sin 2\phi(t)}{4}, & \Omega_{0+}(t) &= -i\dot{\theta}(t) \sin \phi(t) - i \frac{\Gamma \sin 2\theta(t) \sin \phi(t)}{2}, \\ \Omega_{00}(t) &= -i \frac{\Gamma \cos 2\theta(t)}{2}, & \Omega_{0-}(t) &= -i\dot{\theta}(t) \cos \phi(t) - i \frac{\Gamma \sin 2\theta(t) \cos \phi(t)}{2}, \\ \Omega_{--}(t) &= \lambda_-(t) + i \frac{\Gamma \cos 2\theta(t) \cos^2 \phi(t)}{2}, & \Omega_{-0}(t) &= i\dot{\theta}(t) \cos \phi(t) - i \frac{\Gamma \sin 2\theta(t) \cos \phi(t)}{2}, \\ \Omega_{-+}(t) &= -i\dot{\phi}(t) + i \frac{\Gamma \cos 2\theta(t) \sin 2\phi(t)}{4}. \end{aligned} \quad (19)$$

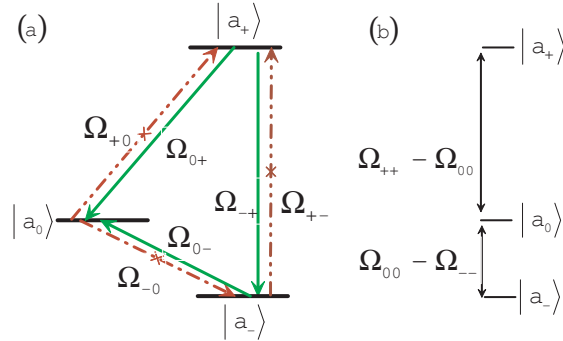


FIG. 3: (a) The resultant energy level diagram of the three-level Λ system when the dissipation effects of the ground states [see Eq. (16)] are considered. (b) The energy difference between the adiabatic states $|a_+(t)\rangle$ and $|a_0(t)\rangle$ ($|a_0(t)\rangle$ and $|a_-(t)\rangle$) in this case is given by $\Omega_{++} - \Omega_{00}$ ($\Omega_{00} - \Omega_{--}$).

Similar to the analysis procedure in Sec. II, we will also use the quantum jump approach to analyse the current model. The resultant energy level diagram is shown in Fig. 3. Interestingly, we find that the effective couplings between the adiabatic states are different from each other. Enlightened by the idea of DQD, we aim at designing the pulses and detuning to cut off some undesirable coupling transitions so that $|a_0(t)\rangle$ becomes the stationary state of the system approximately. Then, even though the initial state is imperfect, the actual state also will follow the evolution of $|a_0(t)\rangle$ closely, thereby transferring the population from $|1\rangle$ to $|3\rangle$ will be achieved efficiently in a short time. According to the DQD, following couplings

$$\Omega_{+0}(t), \Omega_{-0}(t), \Omega_{-+}(t), \Omega_{+-}(t), \quad (20)$$

deviate from our goal, thus, we should make them vanish as much as possible. We can find that $\Omega_{\pm 0}(t)$ can be vanished by setting

$$\frac{2\dot{\theta}(t)}{\sin 2\theta(t)} = \Gamma(t) = \frac{\dot{\Omega}_p(t)}{\Omega_p(t)} - \frac{\dot{\Omega}_s(t)}{\Omega_s(t)} = \frac{d}{dt} \ln \frac{\Omega_p(t)}{\Omega_s(t)}, \quad (21)$$

however, $\Omega_{-+}(t)$ and $\Omega_{+-}(t)$ could not be vanished simultaneously. The next best thing is to nullify one of them so that decreasing the coupling oscillation between the undesirable states $|a_+(t)\rangle$ and $|a_-(t)\rangle$, thereby shortening the evolution time as much as possible. Without loss of generality, we can set $\Omega_{+-}(t)=0$, then $\Delta(t)$ should satisfy following equation

$$\dot{\Delta}(t) = \frac{\dot{\Omega}_0(t)}{\Omega_0(t)} \Delta(t) + \Gamma(t) \cos 2\theta(t). \quad (22)$$

Therefore, the detuning $\Delta(t)$ is designed to cut off the undesirable coupling transitions which plays an important role in the scheme.

Up to now, we have in principle designed the pulses $\Omega_{p,s}(t)$ and the detuning $\Delta(t)$ based on the DQD. Here, we should make some remarks on the design strategies. (1) Generally, the dephasing rate $\Gamma(t)$ is uncontrollable which naturally occurs as a result of collisions or fluctuations of the fields. However, in some cases, $\Gamma(t)$ can be controlled as an effective decay rate by further interactions, see, e.g., Ref. [52]. Therefore, if the form of $\Gamma(t)$ is fixed, the pulses $\Omega_{p,s}(t)$ can be derived with reverse thinking according to the Eq. (21). (2) Once the pulses are fixed, which means the detuning $\Delta(t)$ is fixed according to the Eq. (22). However, we may not be able to get its analytical solution directly from Eq. (22), if the forms of pulses and the dephasing rate are complicated. In this case, the fitting of numerical solution should be applied. Notice that Eq. (21) and Eq. (22) are the primary results to be used in following work.

B. The pulses and the detuning shapes

The scheme is based on the DQD, the dissipative factors play a key role. By “dissipative factors” we mean here a slight deviation of the population with respect to the initial state in the ideal protocol and the dephasing effects of the ground states. In the following, we will take a concrete example to show the usefulness of the dissipative quantum dynamics shortcut design strategy with different dissipative factors. For convenient discussion, we consider a realistic case of a small population in the bare states $|2\rangle$ and $|3\rangle$ for the initial state

$$|\psi(0)\rangle = \sqrt{1 - 2\epsilon^2}|1\rangle + \epsilon(-|2\rangle + |3\rangle), \quad (23)$$

where ϵ is a small deviation constant. Furthermore, we shall take $\Gamma(t)$ as a constant Γ in the Markovian description which was widely discussed in Refs. [9, 10, 47–50], although, in a general non-Markovian case [53–55], it could also depend on time. For the constant dephasing rate Γ , it can easily be shown that the pulses satisfy following equation, taking into account Eq. (21),

$$\frac{\Omega_p(t)}{\Omega_s(t)} = C \exp(\Gamma t), \quad (24)$$

where C is a arbitrary non-zero constant. In addition, according to the standard STIRAP technique, the counterintuitive order of the pump and Stokes pulses can be written as [6–9, 46]

$$\Omega_p(t) = \Omega_{\text{peak}} f\left(\frac{t - \tau_0/2}{T}\right), \Omega_s(t) = \alpha \Omega_{\text{peak}} f\left(\frac{t + \tau_0/2}{T}\right), \quad (25)$$

where Ω_{peak} is the peak Rabi frequency, T is the pulse width, and α is a non-zero scaling parameter, while τ_0 is the delay between pulses which is imposed $\tau_0 > 0$ by the counterintuitive sequence condition. We can find the simplest solutions of Eq. (24) and Eq. (25) for the pulses $\Omega_{p,s}(t)$ are

$$\Omega_p(t) = \Omega_{\text{peak}} \exp(-[(t - \tau_0/2)/T]^2), \Omega_s(t) = \Omega_{\text{peak}} \exp(-[(t + \tau_0/2)/T]^2), \quad (26)$$

where $\tau_0 = \Gamma T^2/2$, C and α are assumed as 1 for simplicity. In the following we will scale all parameters with respect to the width of the pulses,

$$\Omega_{\text{peak}} = \frac{\Omega}{T}, \Gamma = \frac{\gamma}{T}, \tau_0 = \frac{\gamma T}{2} = \tau T, \quad (27)$$

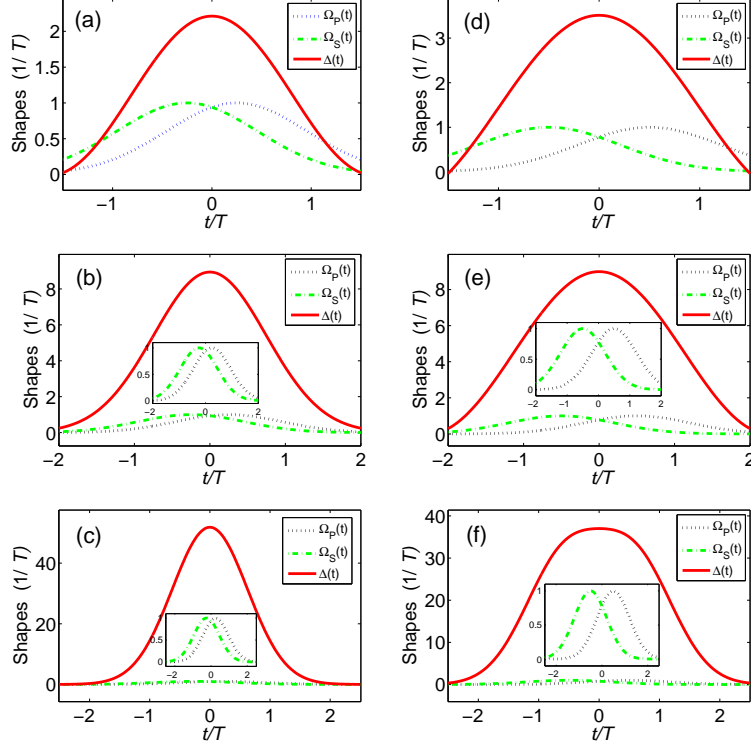


FIG. 4: Evolution in time of the pump and Stokes pulses and the detuning with different dephasing rates within different STIRAP time intervals. For (a), (b) and (c) the dephasing rate $\gamma = 1$: (a) $t_f = 1.5T$, (b) $t_f = 2T$, (c) $t_f = 2.5T$. For (d), (e) and (f) the dephasing rate $\gamma = 2$: (d) $t_f = 1.5T$, (e) $t_f = 2T$, (f) $t_f = 2.5T$. The shapes of the pump and Stokes pulses are based on Eq. (26) with $\Omega = 1$, while the detuning $\Delta(t)$ are plotted according to Eq. (22) by numerical calculations with the boundary condition $\Delta(t_i) = \Delta(t_f) = 0$.

TABLE I: Formal solution for the detuning $\Delta_n(t)$ ($n = a, b, c, d, e, f$), where $\Delta_n(t)$ is the detuning in the Fig. 4(n). The units for $\Delta_{0,1}$ and ω are $1/T$, while that for $\mu_{0,1}$ and $\nu_{0,1}$ are T .

Fitting function	Detuning	Parameters
Fourier $\Delta_0 + \Delta_1 \cos \omega t$	$\Delta_a(t)$	$\Delta_0 = \Delta_1 = 1.12, \omega = 1.92$
	$\Delta_d(t)$	$\Delta_0 = 1.43, \Delta_1 = 2.09, \omega = 1.57$
	$\Delta_e(t)$	$\Delta_0 = \Delta_1 = 4.49, \omega = 1.39$
Gaussian $\Delta_0 e^{-[(t-\mu_0)/\nu_0]^2} + \Delta_1 e^{-[(t-\mu_1)/\nu_1]^2}$	$\Delta_b(t)$	$\Delta_0 = 8.94, \nu_0 = 1.92, \Delta_1 = \mu_{0,1} = \nu_1 = 0$
	$\Delta_c(t)$	$\Delta_0 = 51.83, \nu_0 = 0.88, \Delta_1 = \mu_{0,1} = \nu_1 = 0$
	$\Delta_f(t)$	$\Delta_0 = \Delta_1 = 28.85, \mu_0 = -\mu_1 = 0.6, \nu_{0,1} = 0.9$

so that the system evolution is characterized by a time-scale invariance in the numerical calculations.

Now we start to study the dynamics of the detuning $\Delta(t)$ with different dephasing rates. In Fig. 4, we plot the evolution in time of the pump and Stokes pulses and the detuning with different dephasing rates within different STIRAP time intervals, where we have assumed that the STIRAP time interval is symmetric, $t_f = -t_i$. In the examples of Fig. 4, we can find the shapes of the pump and Stokes pulses and the detuning $\Delta(t)$ are very simple which are feasible for the current experimental techniques [56–59]. From an experimental view point, we give the formal solution for the detuning $\Delta(t)$ with some simple functions by curve fitting as shown in Table I. Moreover, we can find the peak of the detuning $\Delta(t)$ will signally increase with the increase of the STIRAP time interval, and the maximum value of the peak of $\Delta(t)$ is about $51/T$ in the Fig. 4(c). However, the shapes of the detuning $\Delta(t)$ only change slightly for different dephasing rates within the same STIRAP time interval. Up till now, we have successfully designed the pulses and the detuning for different dephasing rates within different STIRAP time intervals.

IV. NUMERICAL ANALYSES

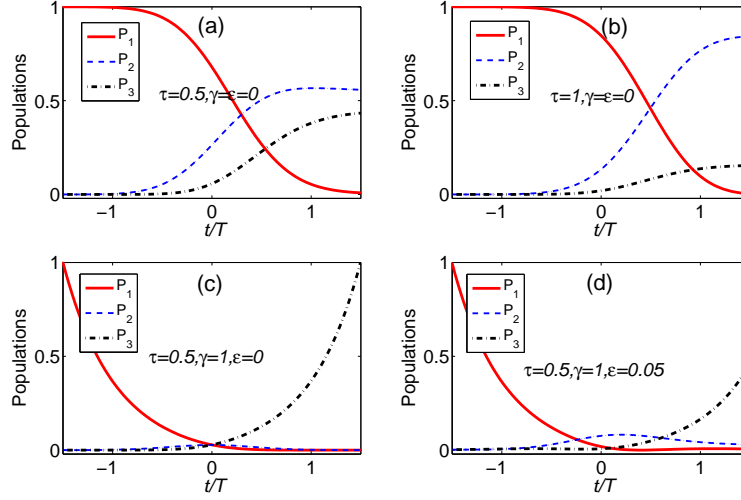


FIG. 5: The time evolution of population P_1 (P_2 , P_3) for the bare state $|1\rangle$ ($|2\rangle$, $|3\rangle$) with the pump and Stokes pulses with different imperfect initial states for the traditional STIRAP process without detuning. The pump and Stokes pulses are based on Eqs. (26-27), while the initial state is based on Eq. (23). For (a) and (b), the initial states are perfectly populated in $|1\rangle$ and the dephasing effects are ignored, the delays τ_0 between pulses are 0.5 and 1, respectively. For (c) and (d), the dephasing rates γ are 1 and the delays τ_0 between pulses are 0.5, the initial state in (c) is perfectly populated in $|1\rangle$, whereas there exists a slight deviation $\varepsilon = 0.05$ from $|1\rangle$ in (d).

Before the elaborating on the performance of the scheme for the complete population transfer from $|1\rangle$ to $|3\rangle$, we will briefly evaluate the performance of traditional STIRAP process with the pump and Stokes pulses which have been shown in Fig. 4 with the help of population engineering. The population for the bare state $|i\rangle$ ($i = 1, 2, 3$) is given through the relation $P_i = |\langle i|\rho(t)|i\rangle|$, where $\rho(t)$ is the density operator of the system at the time t . For convenient discussion, we plot the time evolution of populations for the bare states $|1\rangle$, $|2\rangle$, $|3\rangle$ with four sets of parameters $\{\tau = 0.5, \gamma = \epsilon = 0\}$, $\{\tau = 1, \gamma = \epsilon = 0\}$, $\{\gamma = 1, \tau = 0.5, \epsilon = 0\}$, $\{\gamma = 1, \tau = 0.5, \epsilon = 0.05\}$ in Fig. 5. As shown in Figs. 5(a)-(b), we can find the complete population transfer fails, even though the initial state is perfectly populated in $|1\rangle$ and the dephasing effects are ignored. Figure 5(c) shows a complete population transfer when the initial state is perfectly populated on $|1\rangle$ and there exists the dephasing effect $\gamma = 1$. However, the intermediate state $|2\rangle$ always exists and couldn't be neglected, which may be severe if the excited state $|2\rangle$ will also decay to other states or suffers dephasing during the evolution. Moreover, in Fig. 5(d), the dephasing rate γ is identical to that in Fig. 5(c), whereas there exists a slight deviation of the population with respect to the ideal initial state ($\epsilon = 0.05$). Unfortunately, Fig. 5(d) also shows a invalid population transfer. This means that the traditional STIRAP process is very sensitive to the initial conditions and the deviation of the initial state produces a negative effect. In short, the performances of the traditional STIRAP process are poor with the pump and Stokes pulses which have been shown in Fig. 4 without the detuning $\Delta(t)$.

A. Population engineering

Now, we start to consider the validity of the theoretical analysis by numerical calculation in the following. First, we will study the population engineering of the system with different dissipative factors. Figure 6 shows the time evolution of populations for the bare states $|1\rangle$, $|2\rangle$, $|3\rangle$ with the pump and Stokes pulses and the detuning which have been shown in Fig. 4 for different imperfect initial states. We can easily find that we can fast achieve a complete population transfer from $|1\rangle$ to $|3\rangle$ with the designed pulses and detuning even the initial state is imperfect ($\epsilon \neq 0$). More interestingly, the populations of the state $|2\rangle$ remains negligible all the time in all cases, so the decay of $|2\rangle$ almost has no effect on the evolution of the system. This also means that the evolution of the whole system is completely governed by the adiabatic state $|a_0(t)\rangle$ even the initial state is imperfect. In addition, contrast Fig. 6(a) with Figs. 6(b)-(c), we can find that when the dephasing rate γ is fixed, we can realize the complete population transfer within a shorter time interval for a relatively large deviation $|\epsilon|$. Similar results also can be found by contrasting Fig. 6(d) with Figs. 6(e)-(f). What's more, contrast Fig. 6(a) with Fig. 6(d) (Fig. 6(b) with Fig. 6(e) or Fig. 6(c)

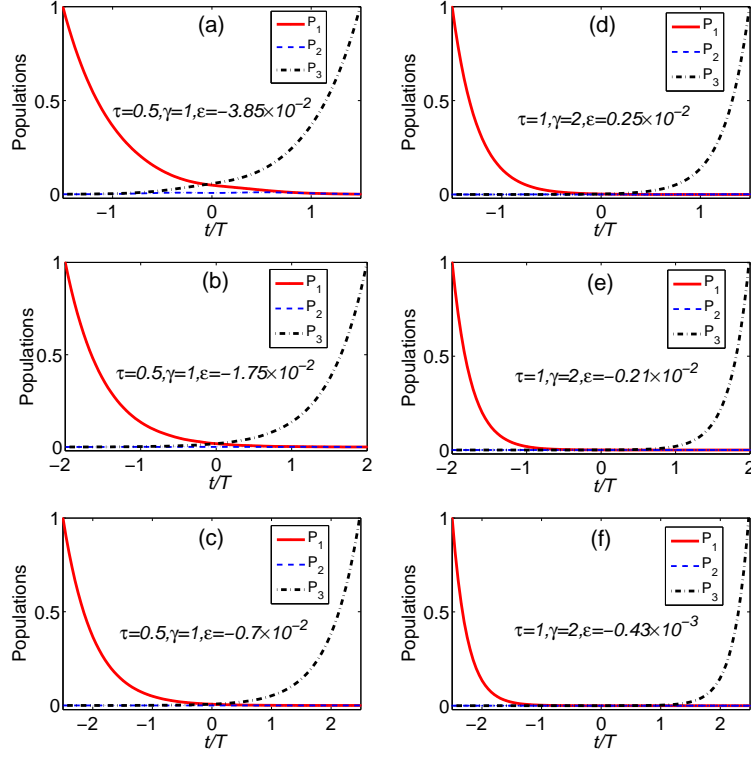


FIG. 6: The time evolution of population P_1 (P_2 , P_3) for the bare state $|1\rangle$ ($|2\rangle$, $|3\rangle$) with the pump and Stokes pulses and the detuning which have been shown in Fig. 4 with different imperfect initial states.

with Fig. 6(f)), we can find that the $|\epsilon|$ will also signally decrease with the increase of γ with the same STIRAP time interval. The reason for these results is that the dissipative factors ϵ and γ are no longer undesirable, actually, they are the important resources to the scheme. In fact, in principle, we can realize the complete population transfer from $|1\rangle$ to $|3\rangle$ within an arbitrarily short time if the dissipative factors are large enough, which is the essential distinction of the scheme comparing with the previous STIRAP or the shortcut technique schemes. However, it should be noted here that, since the system is dissipative, the normalization of the state vector does not need to be conserved [60–62] and it will change in time as shown in Fig. 6.

In any case the normalized states are popular, since they are physically very relevant and can be applied directly in the quantum information processing. It is advisable to keep that the norms of the initial and final state vectors are unity. As a consequence, we will explore in the rest subsection to find an appropriate approach that can remain normalization of the final state. Let us now take a closer look at the normalized final state $|3\rangle$ which is the special form of $|a_0(t_f)\rangle$. This means that if the amplitude of $|a_0(t_f)\rangle$ is 1, we can obtain the normalized final state $|3\rangle$ naturally. A naive choice is seeking for the appropriate parameters to enforce the normalizing, taking into account Eq. (10) and Eqs. (18)–(19). Mathematically, we can get some values for the system parameters (e.g., $\Omega_s, \Omega_p, \Delta(t), \Gamma(t), \epsilon$) with such approach. However, the obvious limitation of this approach is that the solved values generally are scrambled and might be physically irrelevant in practice. In addition, taking no account of the difficulty of calculation, the physical mechanisms behind the parameters are enshrouded in mist, which remains a obstacle to understanding the nature of the evolution.

A different approach for imposing the normalization of the final state is needed. For convenient discussion, we introduce the concept of relative population P_i^r ($i = 1, 2, 3$), where the relative population is defined as $P_i^r = P_i / (P_1 + P_2 + P_3)$. In above theoretical analysis, we confirm that there always exists some optimal parameters to ensure the final state is normalized, e.g., the parameters in Fig. 6. Moreover, as shown in Fig. 6, in the scheme the population in the state $|2\rangle$ is negligible and the evolution of the whole system is completely governed by the adiabatic state $|a_0(t)\rangle$ which only contains states $|1\rangle$ and $|3\rangle$. In other words, so long as we can achieve a complete population transfer within the evolution time, the relative population P_3^r will reach 1. More specifically, due to the inherent role of dissipation in the scheme, the relative population P_3^r will abruptly climb to a high value, and then change slowly to 1 when the system state is approaching to the normalized $|3\rangle$. As a consequence, finding the optimal parameters for imposing the normalization of the final state is equivalent to the solution to a much simpler problem, namely, finding the optimal

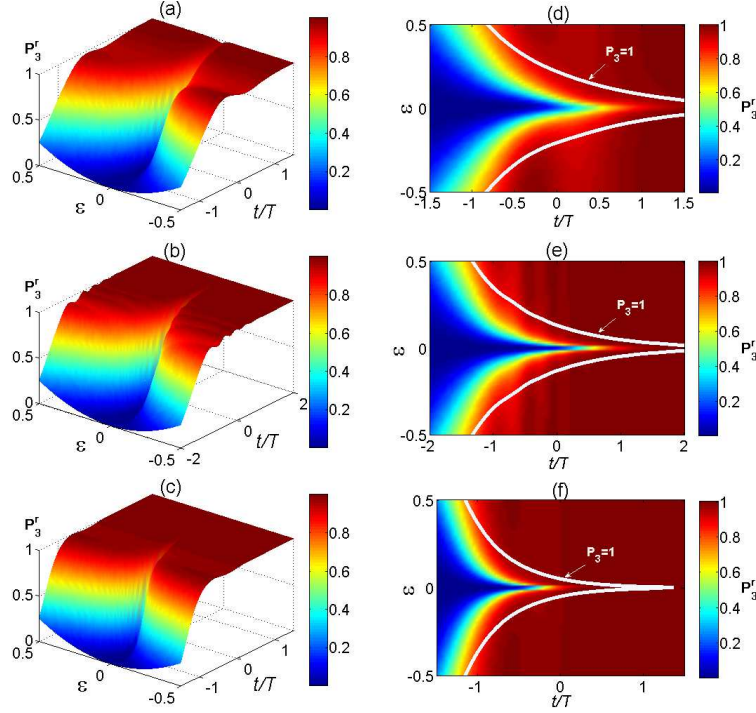


FIG. 7: The relative population P_3^r as a function of t and ϵ with three sets of parameters. The parameters in (a) and (d), (b) and (e), (c) and (f) are identical, corresponding to $(\gamma = 1, t_f = 1.5T)$, $(\gamma = 1, t_f = 2T)$, $(\gamma = 2, t_f = 1.5T)$, respectively. The relative population P_3^r in (a), (b) and (c) with 3D surface, while in (d), (e) and (f) with two-dimensional (2D) plot.

parameters range which will induce the saltation for the relative population P_3^r .

For an intuitive grasp of the approach to normalize the final state, we plot the time evolution of the relative population for the bare state $|3\rangle$ with the deviation coefficient ϵ in the initial state. As shown in Figs. 7(a)-(c), we can get a high relative population P_3^r for a wide range of parameters in the red area. In a sense, if the complete population transfer and robustness are the primary concerns, the scheme is quite efficient, since the relative population P_3^r remains very high (above 0.99) even releasing the requirements. Furthermore, contrast Fig. 7(a) with Figs. 7(b)-(c), we can find the range of parameters for reaching a high relative population P_3^r will signally expand with the increase of γ and the interaction time. Nevertheless, if the normalization of the final state is also important, the optimum parameters for a complete population transfer can be found in the white lines as shown in Figs. 7(d)-(f). It is clear from those figures that the white lines are positioned at the area where the relative population P_3^r increases very quickly and then changes slowly to 1, which is consistent with our deduction. So, we can get the optimum parameters relations between the deviation coefficient ϵ and the evolution time. One can chose the appropriate time to shut down the designed pluses and detuning to obtain the normalized final state $|3\rangle$ according to different ϵ which is dependent on the practical experiment conditions. Interestingly, for a relative large ϵ and γ , the population transfer from $|1\rangle$ to $|3\rangle$ can be obtained in a relative shorter time. For example, in Fig. 7(f) when $\epsilon=0.2$, we can realize the complete population transfer from $|1\rangle$ to $|3\rangle$ and obtain the normalized final state $|3\rangle$ when $t=-0.745T$. In principle, we can realize the complete population transfer within an arbitrarily short time if the dissipative factors are large enough, which is the essential distinction of the scheme comparing with the previous STIRAP or the shortcut technique schemes.

B. Robustness

In order to test the sensitivity of the improved STIRAP scheme to the (simulated) variations in the control parameters, we vary the system parameters around the optimum value for reaching a perfect population transfer. First, we consider the fluctuatings of the pluses parameters. In Fig. 8, the relative population P_3^r and the population P_3 are plotted varying both the peak Rabi frequencies of pulses and the delay between pulses. Figure 8(a) shows that the relative population P_3^r is insensitive to the fluctuations of the pluses, it only varies in the 10^{-3} order of magnitude with the variation of the pluses parameters, which indicates the final state almost is populating on the bare state $|3\rangle$. Nevertheless, the amplitude of $|3\rangle$ is a little sensitive to the fluctuations of the pluses as shown in Fig. 8(b).

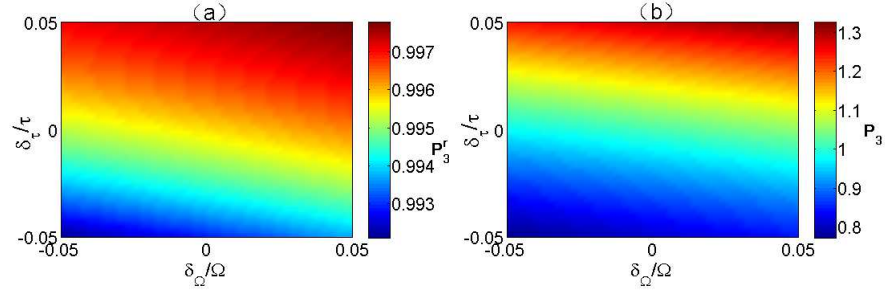


FIG. 8: The relative population P_3^r and the population P_3 vs two relative deviations in the pluses δ_Ω/Ω and δ_τ/τ . The other parameters are $\Omega = 1, \tau = 0.5, \gamma = 1, t_f = 1.5T, \varepsilon = -0.038$, and the detuning with the form of Δ_a as shown in Table I.

The population P_3 will vary from 0.77 to 1.3, and we still can obtain approximately a normalized final state $|3\rangle$ for a moderate fluctuations of the pluses. Moreover, the effect of the relative deviation in the time delay τ will be more obvious than the effect of the relative deviation of the peak Rabi frequency Ω . This is due to the fact the time delay τ is designed carefully as shown in Eq. (26), the relative deviation of τ will induce some undesirable coupling transitions which may affect the normalization of final state slightly. However, the ratio of the Stokes and pumping pluses won't change dramatically in the presence of the amplitude variation of peak Rabi frequency Ω according to Eq. (26), so it naturally has a slight impact on P_3 . We further test the sensitivity of the scheme to the fluctuations of the detuning

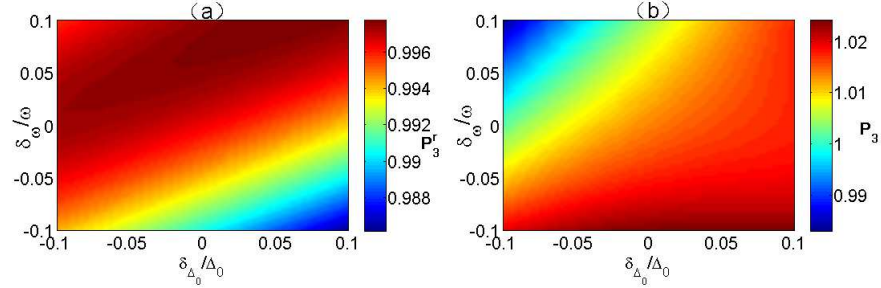


FIG. 9: The relative population P_3^r and the population P_3 vs two relative deviations in the detuning $\delta_{\Delta_0}/\Delta_0$ and δ_ω/ω . The other parameters are $\Omega = 1, \tau = 0.5, \gamma = 1, t_f = 1.5T, \varepsilon = -0.038$, and the detuning with the form of Δ_a as shown in Table I.

Δ_a which is introduced in Table I. Figure 9 evidences out that both the relative population P_3^r and population P_3 are insensitive to the fluctuations of the detuning Δ_a , the perfect P_3^r and population P_3 are obtained even if the detuning is not perfectly matched at the value given in Table I.

In the above discussion, we calculate the sensitivity of the improved STIRAP scheme to the variations in the control parameters by varying one of the protocol parameters in Eq. (2) (i.e., the pluses parameters and single-photon detuning parameters) while keeping all other parameters unchanged. It is nature for us to ask what will happen if all the control parameters vary simultaneously. Table 2 shows some samples of relative population P_3^r and the population P_3 with $\delta_\Omega/\Omega, \delta_\tau/\tau, \delta_{\Delta_0}/\Delta_0$, and δ_ω/ω . We can find the relative population P_3^r is insensitive to the fluctuations of all the control parameters. Nevertheless, the amplitude of $|3\rangle$ is a little sensitive to the fluctuations of the control parameters, and it will vary from 0.7774 to 1.3311. It should be noted that we can approximately obtain the normalized final state $|3\rangle$, if $|\delta_\tau/\tau|$ is small and the other control parameters vary moderately. As discussed above, the scheme shows a good robust feature for potential applications in quantum manipulation.

Table 2. Samples of relative population P_3^r and the population P_3 with corresponding $\delta_\Omega/\Omega, \delta_\tau/\tau, \delta_{\Delta_0}/\Delta_0$, and δ_ω/ω .

δ_Ω/Ω	δ_τ/τ	$\delta_{\Delta_0}/\Delta_0$	δ_ω/ω	P_3^r	P_3
5%	5%	10%	10%	0.9989	1.3311
5%	2.5%	5%	5%	0.9982	1.1812
5%	-2.5%	-5%	-5%	0.9947	0.9435
5%	-5%	-10%	-10%	0.9917	0.8516
2.5%	5%	10%	10%	0.9988	1.3104
2.5%	2.5%	5%	5%	0.9980	1.1607
2.5%	-2.5%	-5%	-5%	0.9944	0.9239
2.5%	-5%	-10%	-10%	0.9913	0.8322
-2.5%	5%	10%	10%	0.9987	1.2694
-2.5%	2.5%	5%	5%	0.9977	1.1212
-2.5%	-2.5%	-5%	-5%	0.9938	0.8864
-2.5%	-5%	-10%	-10%	0.9905	0.7952
-5%	5%	10%	10%	0.9985	1.2494
-5%	2.5%	5%	5%	0.9975	1.1032
-5%	-2.5%	-5%	-5%	0.9934	0.8684
-5%	-5%	-10%	-10%	0.9901	0.7774

C. The dissipation effects of the excited state

In the above discussion, we only consider the dissipation effects of the ground states, the dissipation effects of the excited state $|2\rangle$ has not been taken into account. However, the latter is inevitable in practice and may affect the availability of this method. Thus, we should investigate the influences of the dissipation effects of the excited state, namely, the damping and dephasing of the excited state, on the scheme. Furthermore, we should note that the dissipation effects of the ground states introduced in the Eq. (16) is a good approximation to the master equation by the quantum trajectory approach. When these actual decoherence effects are taken into account, the accurate Lindblad master equation of the whole system can be expressed as [37, 43–45]

$$\dot{\rho} = -i[H_0(t), \rho] - \sum_{j=1,2,3} [L_j \rho L_j^\dagger - \frac{1}{2}(L_j^\dagger L_j \rho + \rho L_j^\dagger L_j)], \quad (28)$$

where $H_0(t)$ is the original Hamiltonian in Eq. (2), and L_j is the so-called Lindblad operator. In current system, the damping of the excited state can be described by the Lindblad operator L_1 , while the dephasing effect can be described by the Lindblad operator L_2 , in addition, the dissipation effects of the ground states can be described by the Lindblad operators L_3 ,

$$L_1 = \sqrt{\Gamma_1}(|1\rangle\langle 2| + |3\rangle\langle 2|), L_2 = \sqrt{\Gamma_2}|2\rangle\langle 2|, L_3 = \sqrt{\Gamma}(|1\rangle\langle 1| - |3\rangle\langle 3|), \quad (29)$$

where Γ_1 represents the branching ration of the damping from level $|2\rangle$ to $|1\rangle$ and $|3\rangle$, Γ_2 denotes the dephasing rate of the $|2\rangle$.

In this subsection, we will concentrate on the influences of the decay rates Γ_1 and Γ_2 on the population transfer, since the influence of Γ has been discussed previously. The relative population P_3^r and the population P_3 vs the decay rates Γ_1 and Γ_2 are given in Fig. 10. It is clear from Fig. 10(a) that the relative population P_3^r is insensitive to the dissipation effects of the excited state, which only varies in the 10^{-3} order of magnitude with the variations of Γ_1 and Γ_2 . Meanwhile, Fig. 10(b) shows that the normalization of final state $|3\rangle$ will be affected slightly by the large dissipation effects of the excited state, moreover, the influence of the dephasing will be more evident than that of the damping. This is due to the fact that the excited state is almost unpopulated during evolution, naturally, the damping rate of the excited state has little effect on the system. Nevertheless, the dephasing will break the superposition of the states [13] according to the quantum trajectory theory. As discussed above, the scheme also shows a good robust feature for potential dissipation effects of the excited state. Therefore, the scheme can work well in various dissipation cases.

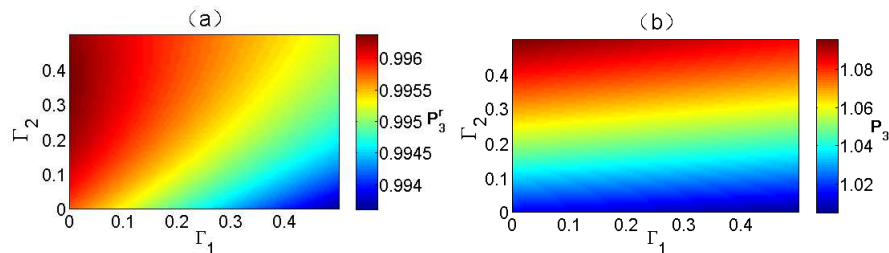


FIG. 10: The relative population P_3^r and the population P_3 vs the decay rates Γ_1 and Γ_2 . The other parameters are the same as shown in the caption of Fig. 6 (a).

V. CONCLUSION

We have proposed a scheme to improve the stimulated Raman adiabatic passage via dissipative quantum dynamics, taking into account the dephasing effects. The complete population transfer can be obtained in a short time with this scheme by the designed pulses and detuning. We investigate the influences of the imperfect initial conditions and the dephasing effects in detail. The numerical simulation results show that the scheme is efficient and robust since the relative population P_3^r remains very high even releasing the requirements. Moreover, the dominant dissipative factors, namely, the dephasing effects of the ground states and the imperfect initial state are no longer undesirable, on the contrary, they are the important resources to the scheme. Interestingly, for a relative large dephasing rate γ and population deviation coefficient ϵ , the population transfer from $|1\rangle$ to $|3\rangle$ can be obtained in a relative shorter time. That is, we can realize the complete population transfer within an arbitrarily short time if the dissipative factors are large enough. This is the essential distinction of the scheme comparing with the previous STIRAP or the shortcut technique schemes. On the other hand, the effects of variations of the control parameters and various dissipation effects are also discussed in detail. The results show that the scheme is insensitive to moderate fluctuations of experimental parameter and the relatively large dissipation effects of the excited state, a high fidelity can be reached for a wide range of parameters. Therefore, the scheme could provide more choices for the realization of the complete population transfer in the strong dissipative fields where the standard STIRAP or shortcut schemes are invalid.

Furthermore, we should note that any quantum system whose Hamiltonian is possible to be simplified into the form in Eq. (17) (the basic for the simplified Hamiltonian can be arbitrary dressed states, as long as, the dressed states satisfy the the orthogonality relation and closure relation), the scheme can be implemented straightforward. This might lead to a useful step toward realizing fast and noise-resistant quantum information processing for multi-qubit systems in current technology. Furthermore, one may also try adding some dissipative factors to make the undesirable coupling transitions vanish for a more generic system. Moreover, in above discussion, we consider the damping effect in the Markovian description for convenience, since some parameters (e.g., $\Gamma(t)$) can be considered as the constant. However, in a general non-Markovian case [53–55], these parameters could also depend on time, then, the dynamics of the system will be complicated and the evolution speed and the robustness of the scheme will also be changed signally. In fact, such issue is interesting and attractive, the dynamical aspect of quantum open systems is also the field where the further extensions of this work may be explored.

Acknowledgment

This work was supported by the National Natural Science Foundation of China (NSFC) under Grants No. 11575045 and No. 11374054, and the Major State Basic Research Development Program of China under Grant No. 2012CB921601.